



## Development and Design of Portable 1 Phase Spot Welding Machine

Ipfung Kurniawan, Pujono\*, Fendy Aldianto, Daffa Pandora Althafadilah, Joko Setia Pribadi, Dian Prabowo

*Diploma Program in Mechanical Engineering, Politeknik Negeri Cilacap, Jl. Dr. Soetomo No. 1 Karangcengis Sidakaya, Cilacap 53212 Indonesia*

\*Corresponding author: [poejono07@gmail.com](mailto:poejono07@gmail.com)

### ARTICLE INFO

Received 03/02/2025  
Revision 14/03/2025  
Accepted 29/03/2025  
Available online 30/04/2025

### ABSTRACT

The design method used as an approach in designing portable spot welding machines is the VDI 2222 design method. Working drawings use ISO standards and the design application used is solidworks. From the design method used as an approach in designing portable spot-welding machines, the results of image documents in the form of working drawings are obtained which will then be used in the production process. The result of maximum stress calculation result of the frame used is  $0,301 \text{ N/mm}^2 \leq \sigma_{izin} = 166,67 \text{ N/mm}^2$ , therefore the results obtained show that the elbow profile size  $40 \times 40 \times 2 \text{ mm}$  is confirmed to be safe to withstand the given load. The spring calculation above  $\tau_{max} = 27,07 \text{ kg/mm}^2 \leq \tau_a = 65 \text{ kg/mm}^2$ , therefore the results obtained show that the spring with a winding diameter of 7 mm and a wire diameter of 1.2 mm is certainly safe to withstand the given load.

**Keywords:** *design, portable spot welding, tensile test*

### 1. INTRODUCTION

Spot welding is a method used to join metals by creating a spot weld. This technique is commonly employed in large industries, particularly in the automotive and motorcycle sectors, and is primarily used for joining thin sheets of metal. Spot welding is a type of electrical resistance welding that involves the connection of metal plates at specific points, where low voltage current flows between the electrodes. This causes the areas of metal in contact to heat up due to the electrical current, raising the temperature to the level required for welding. The process involves applying pressure with two electrodes that move up and down to fuse the metal together at the designated spots [1].

Mild steel is a type of carbon steel with a carbon content of less than 0.3%. It is commonly used in construction and machine components, such as vehicles, house fences, and various other applications. Mild steel is characterized by its relatively low hardness, high toughness, and ease of welding [2].

Stainless steel, on the other hand, is a type of steel known for its resistance to corrosion at both high and low temperatures. It has a low carbon content and is primarily composed of chromium, which provides its corrosion resistance, along with added nickel. Some stainless-steel types also include other elements such as phosphorus, manganese, silicon, and molybdenum. Generally, stainless steel is divided into three main categories: austenitic, martensitic, and ferritic stainless steel [3].

In previous studies that analyzed the impact of welding time and spot-welding current strength on the tensile strength of stainless steel 304, tests conducted using the Krisbow DN-10-01 spot welding machine yielded results indicating that increased current and longer welding time enhance the strength of the welded joints. This improvement occurs because the increased heat better melts the material, resulting in a stronger weld [4].

In contrast to these earlier studies, this research focuses on designing a one-phase portable spot-welding machine and conducting tensile tests on

welding specimens. The primary objective of this study is to develop a one-phase portable spot-welding machine and perform tensile testing on welded specimens made of mild steel and stainless-steel plates.

## 2. METHODOLOGY

The design research method and tensile testing of welding specimens for the portable 1-phase spot welding machine involve several stages. Figure 1 illustrates the research methodology in a flowchart format.

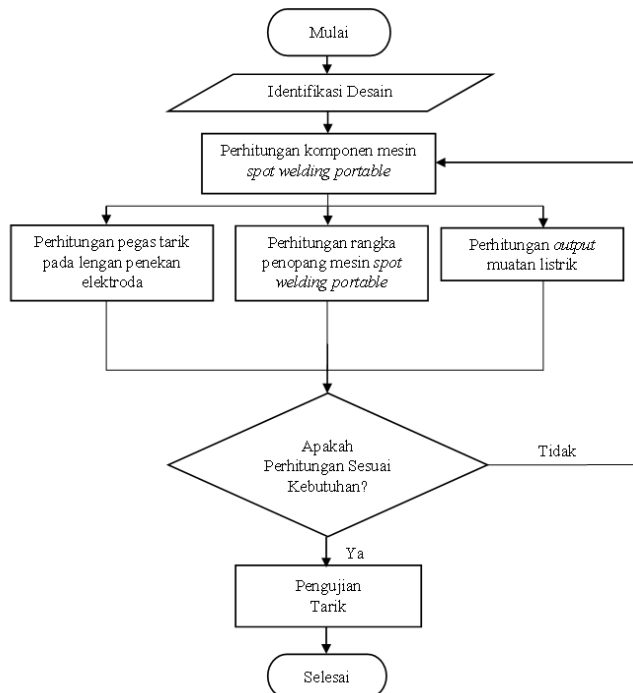


**Figure 1.** Research methodology

The research stages are conducted in a sequential manner. It begins with literature reviews and field studies, followed by the design process, preparation of tools and materials, and then the welding process. If the welding is successful, the research advances to the testing stage, which includes tensile tests, data analysis, discussions, and conclusions.

In this study, two types of test specimens were utilized, each differing in their characteristics and chemical composition.

- The mild steel used is a sheet plate with a thickness of 0.8 mm, formed in accordance with the ASME IX standard.
- The stainless steel used is also a sheet plate with a thickness of 0.8 mm, formed according to the ASME IX standard.

The arrangement of the lap joint plates adheres to the AWS D8.9-97 standard, as illustrated in Figure 2.

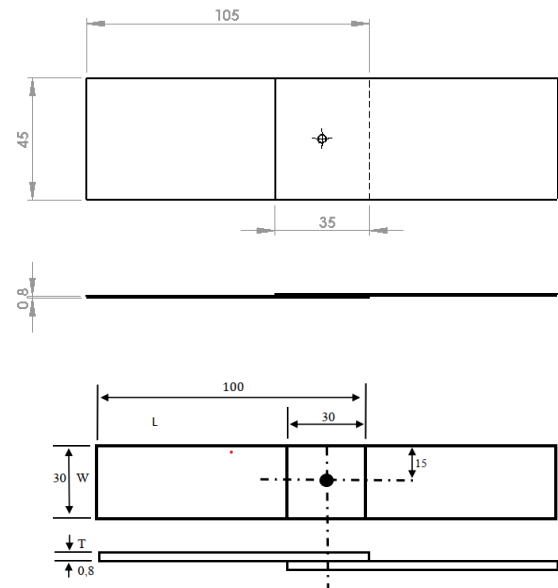


**Figure 2.** The lap joint plates are arranged in accordance with the AWS D8.9-97 standard

## 3. RESULTS AND DISCUSSION

### 3.1 Design process

The machine box is a compartment that serves to store and protect the main components of a portable spot-welding machine, including a transformer, timer control, cable, and cooling fan. The machine box design is illustrated in Figure 3.

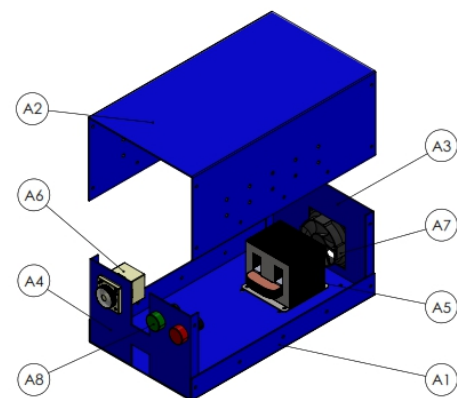


**Figure 3.** Design of the machine box

The descriptions of each component of the engine box are provided in Table 1.

**Table 1.** Part of machine box

No	Part name	Material
A1	Base box	Mild steel
A2	Top cover of box	Mild steel
A3	Back cover	Mild steel
A4	Front cover	Mild steel
A5	Transformer	Standard
A6	Time control	Standard
A7	Cooling fan	Standard
A8	Indicator lamp	Standard

The arm driver consists of two primary components: the presser arm and the drive pedal. The presser arm serves as an electrode holder, while the drive pedal enables the movement of the presser arm up and down. The design of the arm driver is illustrated in Figure 4

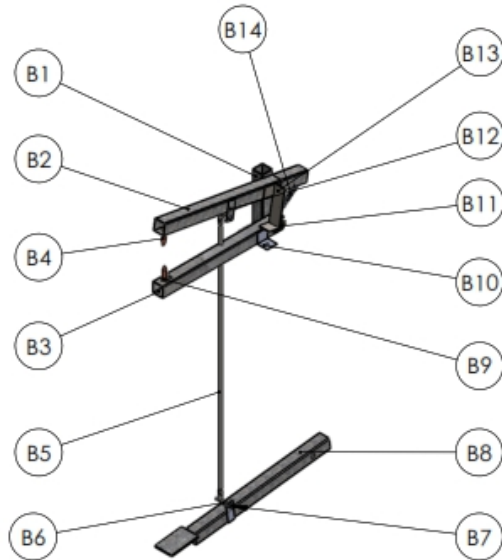


Figure 4. Design of the electrode arm driver

The details of each component of the arm drive are listed in Table 2.

Table 2. Arm drive part

No	Part name	Material
B1	Arm support	Galvanized
B2	Pressing arm	Galvanized
B3	Fixing arm	Galvanized
B4	Electrode	Copper
B5	Connector	Mild-steel
B6	Puller lever	Mild-steel
B7	Connector pin	Mild-steel
B8	Pedal	Galvanized
B9	Insulator	Ebonite
B10	Arm bracket	Mild-steel
B11	Limit switch	Standard
B12	Puller lever bracket	Mild-steel
B13	Limit switch pusher	Mild-steel
B14	Return spring	Wire

### 3.2 Frame calculation

The support rod designed to bear the centralized load is constructed from the front workbench profile. We can describe it using a calculation formula to ensure the strength and safety of the profile used for the portable spot-welding machine. The loading characteristics of the rod profile are illustrated in Figure 5.

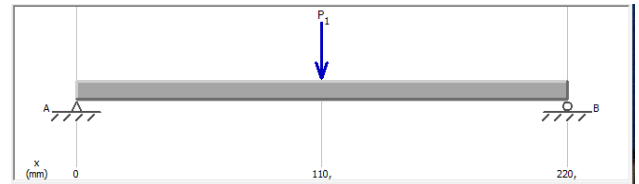


Figure 5. Loading profile

To calculate the force acting on the bar profile, follow these steps.

$$\text{Mass } m = 2.14 \text{ kg and } g = 9.8 \text{ m/s}^2$$

$$F = mg$$

The total mass includes 1 pusher lever, 2 pedal brackets, 2 connectors, 1 pedal, 1 electrode, and a cable. The compressive load is specified.

$$m = 0.212 + 2(0.015) + 2(0.01) + 0.465 + 0.026 + 0.40 + 1.00 = 2.153 \text{ kg}$$

$$F = mg = 2.153(9.80) = 21 \text{ N}$$

The calculated force acting on the front work table profile is 21 N.

### Calculating reaction force

The reaction force  $R_A$  and  $R_B$  can be calculated with the following steps.

$$\sum M_A = 110P - 220R_B = 0$$

$$R_B = 10.5 \text{ N}$$

$$\sum M_B = -110P + 220R_A = 0$$

$$R_A = 10.5 \text{ N}$$

The calculation results for the reaction force from the front workbench profile are  $R_A = 10.5 \text{ N}$  and  $R_B = -10.5 \text{ N}$ , as shown in Figure 6.

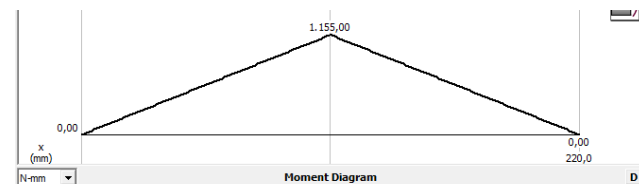


Figure 6. Bending moment diagram

The frame serves as the primary support for the portable spot-welding machine's box. The frame assembly design is illustrated in Figure 7.

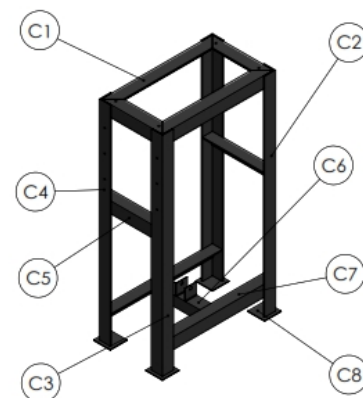


Figure 7. Frame assembly design

The description of each part of the frame assembly is explained in Table 3.

**Table 3.** Frame assembly part

No	Part name	Material
C1	Engine box stand	Mild steel
C2	Rear leg	Mild steel
C3	Left front leg	Mild steel
C4	Right front leg	Mild steel
C5	Frame leg support 1	Mild steel
C6	Pedal stand	Mild steel
C7	Frame leg support 2	Mild steel
C8	Foot base plate	Mild steel

### Calculating the moment of inertia of iron rod

The moment of inertia of the rod can be calculated if the cross-section of the rod is known. The cross-section of the angle iron rod is shown in Figure 8.

Given  $b_1 = 40$  mm,  $h_1 = 2$  mm,  $b_2 = 2$  mm,  $h_2 = 38$  mm, and modulus Elastisitas  $E = 210000$  N/mm<sup>2</sup>, the momen of inertia is:

$$I_{xx} = \frac{1}{12}bh^3$$

$X_1 = 20$  mm,  $X_2 = 1$  mm

$$A_1 = b_1 \cdot h_1 = 40(2) = 80 \text{ mm}^2$$

$$A_2 = b_2 \cdot h_2 = 1(38) = 76 \text{ mm}^2$$

$$A_{tot} = A_1 + A_2 = 80 + 76 = 156 \text{ mm}^2$$

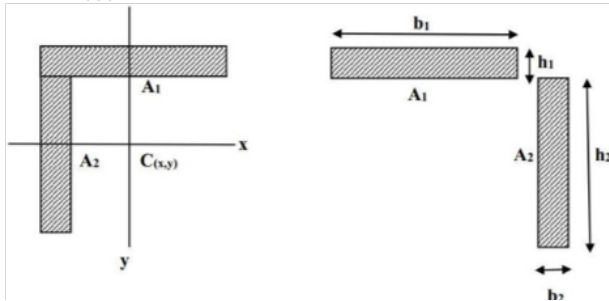


**Figure 8.** Cross section of iron plate

$$I_{x1} = \frac{1}{12}b_1h_1^3 = \frac{1}{12}(40)(2)^3 = 26.67 \text{ mm}^4$$

$$I_{x2} = \frac{1}{12}b_2h_2^3 = \frac{1}{12}(2)(38)^3 = 9145.33 \text{ mm}^4$$

Total moment of inertia:

$$I_1 = I_{x1} + (A_1 \cdot x_1^2) = 26.67 + 80(20)^2 = 32026.67 \text{ mm}^4$$

$$I_2 = I_{x2} + (A_2 \cdot x_2^2) = 9145.33 + 80(1)^2 = 9225.33 \text{ mm}^4$$

$$I_{tot} = I_1 + I_2 = 32026.67 + 9225.33 = 41252 \text{ mm}^4$$

The moment of inertia for iron plate is 41252 mm<sup>4</sup>.

### 3.3 Testing

When conducting research, it is essential to prepare the necessary tools. The tools used in this study include:

1) Portable 1-phase spot welding machine

The welding process was carried out using a portable 1-phase spot welding machine. This machine is capable of welding plates with a maximum thickness of 1 mm and operates on a single-phase electric power source. It achieves an average current value of 250A during the welding process.

2) Tensile testing equipment

A tensile testing tool is essential for determining the mechanical properties, particularly the strength, of a material subjected to tensile forces. In this study, a UTM (Universal Testing Machine) of the Tensilon type, RTI-1310, was used. This machine features a maximum load capacity of 10 kN and a maximum speed of 500 mm/min. The tensile strength tests were conducted at the Cilacap State Polytechnic Testing Laboratory.

3) Testing aids

Various tools were utilized throughout the research process, proving to be very helpful to the study. These tools include:

- A cutting machine for cutting stainless steel and mild steel sheets to specified sizes.
- An ampere clamp for measuring the output current of the spot-welding machine.
- Pliers and plate scissors.
- Measuring tools such as rulers, markers, pencils, calipers, and digital scales.
- Autosol and sandpaper for finishing touches.

### 3.4 Welding process

Spot-welding operates by transforming the alternating current voltage from 220V to a lower voltage of 2V to 12V using a transformer in the welding machine. This transformation increases the current to a point where it generates sufficient heat.

The plates to be welded are clamped together at the joint using a pair of copper alloy electrodes. At this point, a high electric current flow through the clamped area for a brief period. As the electric current passes between the two electrodes and through the metal, heat is generated due to electrical resistance. This heat causes the metal at the clamped area to melt, thereby forming a connection [5].

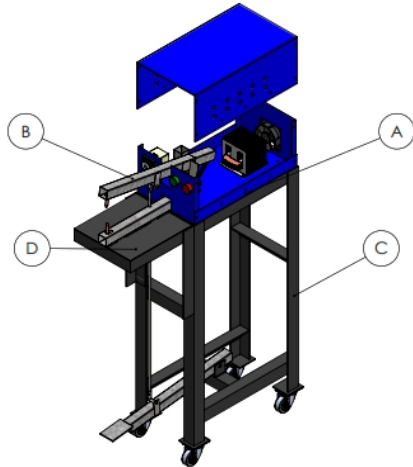
### 3.5 Tensile testing process

A standard method for determining the mechanical properties of a material involves conducting tensile or shear tests. In the tensile testing process, a static force is applied gradually until the specimen finally breaks [6]. The strength of the material is typically measured by the maximum force that the specimen can withstand per unit area.

$$\tau = \frac{F_m}{A_0}$$

Where,  $\tau$  is shear stress ( $\text{N/mm}^2$ ),  $F_m$  is maximum force (N), and  $A_0$  is initial cross-sectional area ( $\text{mm}^2$ ).

This study presents a design plan for a one-phase portable spot-welding machine and provides tensile test data for welding specimens made from mild steel and stainless-steel plates. The design plan is used to determine the shape of the tool or machine being manufactured, as illustrated in Figure 9.



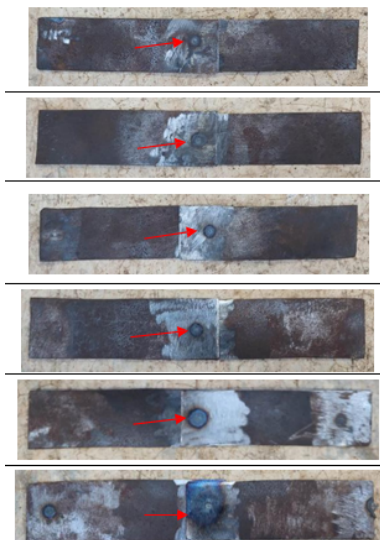
**Figure 9.** Portable spot-welding machine design

Table 4 explains the descriptions of each part of the portable spot-welding machine.

**Table 4.** Portable spot-welding machine parts

No	Part name	Quantity
A	Machine box	1
B	Arm drive	1
C	Frame assembly	1
D	Workbench	1

Tensile testing is performed to measure shear stress, denoted in units of  $\text{N/mm}^2$ . This testing is conducted on mild steel specimens, which are illustrated in Figure 10.



**Figure 10.** Test specimens

The results of the welding joint tests are presented in Table 5.

**Table 5.** Test result data

No	Plate type	Plate thickness (mm)	Time (s)	Output current (A)	Tensile testing (MPa)
1	Mild steel	0.4	4	250	4.71
			8	250	5.06
			12	250	13.04
2	Mild steel	0.8	4	250	1.03
			8	250	2.24
			12	250	5.45

If represented graphically, the impact of welding time on the tensile strength (specifically shear strength) of welded joints can be illustrated in Figures 11 and 12.

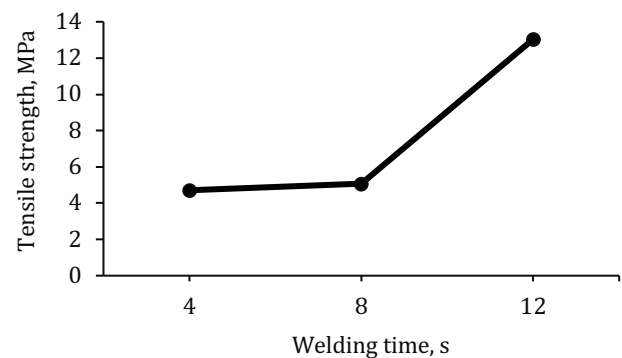


**Figure 11.** Tensile test graph for a 0.4 mm mild steel plate

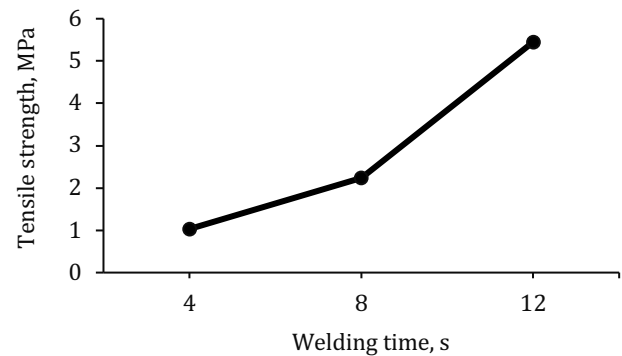


**Figure 12.** Tensile test graph for a 0.8 mm mild steel plate

From Figure 12, it can be observed that, in general, as the current strength and welding time increase, the average tensile strength of the welded joints also rises. This trend is evident across the three-time variations examined (4 seconds, 8 seconds, and 12 seconds) with a constant current strength. The increase in tensile shear strength indicates that higher heat input—resulting from the changes in current strength and welding duration—leads to a larger diameter of the spot weld nugget. This larger nugget size is likely responsible for the increased tensile shear force.

The maximum tensile shear strength is recorded at a current strength of 250A and a welding time of



12 seconds, corresponding to a tensile shear force of 13.4 N/mm<sup>2</sup>. This represents the highest tensile shear force among the various welding parameter combinations tested. Additionally, while the average tensile strength increases with longer welding times at a constant current of 250A, the greatest tensile strength is achieved specifically at the 12-second mark. This suggests that the optimal heat input at this point produces a joint characterized by a larger weld nugget size, which results in a greater tensile force.

#### 4. CONCLUSION

The design results yielded detailed drawings for a portable spot-welding machine with dimensions of 1200 x 600 x 220 mm. According to the table and graph of the tensile test results, it was observed that longer welding times lead to higher tensile stress values. Furthermore, a plate thickness of 0.4 mm exhibits a greater tensile stress value compared to a plate thickness of 0.8 mm when subjected to the same welding time. Overall, the test results indicate that the welding time is a significant factor influencing the outcomes of spot-welding.

#### ACKNOWLEDGMENTS

In this section, we express our gratitude to those third parties, other than the authors, who played a significant role in preparing the paper. Additionally, we acknowledge the sources of research funding in this section.

#### REFERENCES

1. Nowak WJ. Control of kinetics of plasma assisted nitriding process of Ni-base alloys by substrate roughness. *Adv Manuf Sci Technol*. 2020;0(0):99–108.
2. Lakhtin YM. High-temperature nitriding. *Met Sci Heat Treat*. 1991;33(2):124–30.
3. Nayak BB, Kar OPN, Behera D, Mishra BK. High temperature nitriding of grey cast iron substrates in arc plasma heated furnace. *Surf Eng*. 2011;27(2):99–107.
4. Roliński E, Konieczny A, Sharp G. Influence of nitriding mechanisms on surface roughness of plasma and gas nitrided/nitrocarburized gray cast iron. *Heat Treat Prog*. 2007;7(2):39–46.
5. Wolowiec-Korecka E, Michalski J, Kucharska B. Kinetic aspects of low-pressure nitriding process. *Vacuum*. 2018 Sep;155(June):292–9.
6. Yamaguchi S, Ichikawa T, Wang Y, Nakagawa Y, Isobe S, Kojima Y, et al. Nitrogen Dissociation via Reaction with Lithium Alloys. *ACS Omega*. 2017;2(3):1081–8.
7. Feichtinger H, Zheng X, Rennhard C. Measurements of nitrogen solubility in iron and iron-nickel alloys, using a new temperature gradient method. *Steel Res*. 1990 Jan;61(1):26–9.